coatings

MDPI

Communication

Modeling of Ionizing Radiation Effects for Negative Capacitance Field-Effect Transistors

Yongguang Xiao [1,2,*], Xianghua Da [1,2], Haize Cao [1,2], Ke Xiong [1,2], Gang Li [1,2] and Minghua Tang [1,2]

[1] Key Laboratory of Key Film Materials, Application for Equipments (Hunan Province), School of Material Sciences and Engineering, Xiangtan University, Xiangtan 411105, China
[2] Hunan Provincial Key Laboratory of Thin Film Materials and Devices, School of Material Sciences and Engineering, Xiangtan University, Xiangtan 411105, China
* Correspondence: ygxiao@xtu.edu.cn

Abstract: A theoretical model for simulating ionizing radiation effects on negative capacitance field-effect transistors (NCFETs) with a metal–ferroelectric–insulator–semiconductor (MFIS) structure was established. Based on the model, the effects of total ionizing dose (TID) and dose rate on the surface potential, ferroelectric capacitance, voltage amplification factor, and transfer characteristics of NCFETs were investigated. The simulation results demonstrated that, with the increase in total dose, the curves of surface potential versus gate voltage and driving current versus gate voltage shift left significantly, resulting in the point of voltage amplification shifting left. Meanwhile, with the increase in dose rate, the amplitude of both the surface potential and driving current decreases slightly. Meanwhile, the derived result indicated that relatively thin ferroelectric thickness can effectively reduce the effect of TID. It is expected that this model can be helpful for analyzing the radiation effects of NCFETs.

Keywords: negative capacitance; ionizing radiation effect; TID; dose rate effect; field-effect transistor

Citation: Xiao, Y.; Da, X.; Cao, H.; Xiong, K.; Li, G.; Tang, M. Modeling of Ionizing Radiation Effects for Negative Capacitance Field-Effect Transistors. *Coatings* **2023**, *13*, 798. https://doi.org/10.3390/coatings13040798

Academic Editor: Torsten Brezesinski

Received: 23 March 2023
Revised: 10 April 2023
Accepted: 15 April 2023
Published: 20 April 2023

1. Introduction

Since Salahuddin first introduced the concept of the negative capacitance field-effect transistor (NCFET) in 2008 [1], the investigation into the electrical properties [2–5] of the ferroelectric negative capacitance effect and its theoretical mechanism [6–8] has yielded significant advancements in the field. Furthermore, these studies have facilitated experimental research into NCFET and have contributed to its characterization as a device with exceptional performance [9–13]. Previous reports have demonstrated NCFETs' potential for circuit testing [14,15], further cementing its position as a promising technology for future electronic applications. Negative capacitance field-effect transistors (NCFETs) can break the Boltzmann limit, effectively solving the contradiction between low power consumption and high performance of transistors, and can significantly enhance the performance of integrated circuits. However, microelectronic devices can be damaged by radiation from high-energy particles or rays in space, which can degrade the performance of the device or even make it invalid. The total ionizing dose (TID) response as well as the dose rate effect are important factors affecting the reliability of devices in the space environment. In recent years, the effect of ionizing radiation on ferroelectric field-effect transistors (FeFETs) has been a hot research topic. There are many theoretical models concerning the radiation effect for FeFETs. For instance, a numerical model describing the leakage characteristics of ferroelectric thin films under ionizing radiation has been developed by Sun et al. [16]. They modified the trap-controlled space charge-limited conduction mechanism by taking into account the radiation-induced charge carrier and relative dielectric constant variations. Chong et al. [17] have investigated the TID effect in oxide/source overlapped SOI (silicon-on-insulator) TFETs (tunneling field-effect transistors). Ray et al. [18] studied the TID

response of SOI-FinFET with linear gate work function modulation. Cui et al. [19] investigated the TID effect of 22 nm bulk silicon nFinFETs with different bias conditions. However, there are few research works on the radiation response of NCFETs at present [20,21]. In this work, a theoretical model of ionizing radiation effects for NCFETs was proposed to investigate the surface potential, ferroelectric capacitance, voltage gain, and drain current by considering the radiation-induced trapped charges, the fixed charges generated in the ferroelectric and insulating layers, and the interfacial charges generated between the insulating layer and the silicon substrate caused by TID and dose rate effects.

2. Physical Model

First, the MFIS NCFET structure considered in this work is shown in Figure 1. For this structure, the potential balance equation for classical MOSFETs can be written as [22]

$$V_g = V_{fb} + V_F + \psi_{ox} + \varphi_s, \tag{1}$$

where V_{fb} is the flat-band voltage and V_F and ψ_{ox} are the potentials dropped across the ferroelectric (FE) layer and the oxide layer, respectively. $\psi_{ox} = Q/C_{ox}$, where Q and C_{ox} are the charge density and the oxide capacitance per unit area, respectively. In order to obtain V_F, one needs to invoke the Landau–Devonshire theory, relating the electric field (E) and the polarization (P), which is expressed as

$$E = 2\alpha P + 4\beta P^3 + 6\gamma P^5, \tag{2}$$

where, α, β, and γ are the Landau coefficients [23]. According to the integrated derivation of the Landau–Khalatnikov (LK) theory and Gibb's free energy, from [24], one can obtain

$$V_F = 2\alpha d_{fe} Q + 4\beta d_{fe} Q^3 + 5\gamma d_{fe} Q^5, \tag{3}$$

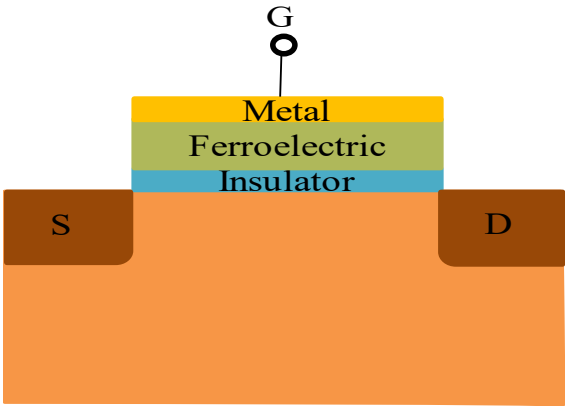

Figure 1. Schematic of an MFIS-NCFET structure.

The term of d_{fe} stands for the ferroelectric thickness. According to Equation (3), C_{fe} can be expressed as [25]

$$C_{fe} = \partial Q/\partial V_F = 1/(2d_{fe}\alpha + 12d_{fe}\beta Q^2 + 25\gamma d_{fe} Q^4), \tag{4}$$

The insulating layer in the device structure is SiO_2, the ferroelectric material is strontium bismuth tantalite ($SrBi_2Ta_2O_9$, SBT), and the channel material is assumed to be silicon. We take SBT as the example of which of the exact coefficients are expressed as $\alpha = 2.03 \times 10^5$ (T-620) m/F, $\beta = 3.75 \times 10^9$ m^5/(F·C^4), and $\gamma = 0$. In the MOS (metal oxide semiconductor) structure, considering the radiation conditions, V_{fb} can be expressed as [26]

$$V_{fb} = \varphi_{ms} - q(\Delta N_{fe} + \Delta N_{it} + \Delta N_{ox})/C_{stack}, \tag{5}$$

where φ_{ms} is the work function difference between the gate and the substrate. $C_{stack} = (C_{ox}{}^{-1} + C_{fe}{}^{-1})^{-1}$, $C_{ox} = \varepsilon_{ox}/d_{ox}$, where ε_{ox} is the permittivity of the oxide layer and d_{ox} is the oxide layer thickness. ΔN_{fe} is the number of radiation-induced trapped charges in the FE layer. ΔN_{it} is the number of radiation-induced oxide–silicon interface trapped charges. ΔN_{ox} is the number of radiation-induced trapped charges in the insulator layer. Under radiation conditions, excess electron–hole pairs generated per unit volume in the silicon substrates are [27] $\Delta n = g_{si} D \tau_r$, where

$$\tau_r = (-N_d + \sqrt{N_d{}^2 + 4 g_{si} N_d \tau D})/(2 g_{si} D), \tag{6}$$

where N_d is the doping concentration, g_{si} is the carrier generation rate conversion factor [carrier = (m^3·rad)] in the silicon substrate, D is the incident dose rate (rad/s), τ is the lifetime of minority carriers before radiation, and τ_r is the lifetime of minority carriers after radiation. The one-dimensional continuity equation for uniform ionizing radiation-induced charges for the valence band hole concentration in the ferroelectric and insulator layers can be written as [28]

$$\Delta N_{fe} = (1/d_{fe}) \int_0^{d_{fe}} p_{t-fe} \cdot x dx, \tag{7}$$

$$\Delta N_{ox} = (1/d_{ox}) \int_0^{d_{ox}} p_{t-ox} \cdot x dx, \tag{8}$$

where p_{t-fe} and p_{t-ox} are the concentration of radiation-induced trapped holes in the FE and oxide layer, respectively. The number of radiation-induced oxide–silicon interface trapped charges can be written as [29]

$$\Delta N_{it} = (1/2) N_{it} \sigma_{it} N_{DH} \sigma_{DH} g_{si} f_{it} d_{ox}^2 D t, \tag{9}$$

where N_{it} is the interface trap, σ_{it} is the interface capture cross-section, N_{DH} is the density of hydrogen-containing defect cavity traps in the insulator layer, σ_{DH} is the cross section of hydrogen-containing defect traps, and f_{it} is the electron–hole separation probability at the interface under irradiation.

According to Sze's model, considering the irradiation conditions, the relationship between Q and φ_s can be described as [30]

$$\begin{aligned} Q(\varphi_s) &= -\mathrm{sign}(\varphi_s) \times \tfrac{\sqrt{2}\varepsilon_s}{\beta L_D} \\ &\left[\left(\tfrac{n_i^2}{(N_d+\Delta n)^2} \left(\mathbf{e}^{-\beta\varphi_s} + \beta\varphi_s - 1 \right) + \left(\mathbf{e}^{\beta\varphi_s} - \beta\varphi_s - 1 \right) \right)^{1/2} \right] \end{aligned} \tag{10}$$

Here, L_D is the Debye length, N_d stands for the majority carrier concentration, and n_i is the intrinsic carrier concentration. β is defined as $\beta = q/(kT)$, with the Boltzmann constant k, the electronic charge q, and temperature T. The current from source to drain for MFIS-NCFET can be obtained by [31]

$$I_d = q\mu \frac{W}{L} \int_0^{V_{DS}} \int_{\varphi_B}^{\varphi_s} \frac{n_i^2 \mathrm{e}^{-\beta(\varphi - V)}}{(N_d + \Delta n)\xi(\varphi_s, V)} \mathrm{d}\varphi \mathrm{d}V, \tag{11}$$

Here, $\varphi_B = (kT/q) ln((N_d + \Delta n)/n_i)$, and $\xi(\varphi_s, V)$ can be expressed as

$$\begin{aligned} &\xi(\varphi_s, V) = \sqrt{\tfrac{2(N_d+\Delta n)kT}{\varepsilon_s}} \\ &\left[\left(\mathrm{e}^{\beta\varphi} - \beta\varphi - 1 \right) + \tfrac{n_i^2}{(N_d+\Delta n)^2} \mathrm{e}^{\beta V} \left(\mathrm{e}^{-\beta\varphi} + \beta\varphi \mathrm{e}^{-\beta V} - 1 \right) \right]^{1/2}. \end{aligned} \tag{12}$$

3. Results and Discussion

To investigate the effect of TID on the performance of the NC-MFIS-FETs, we firstly plotted the curves of φ_s–V_g under different total doses (from 0 rad to 2 Mrad) in Figure 2a. The ferroelectric thickness was assumed to be 35 nm [16] and the dose rate was kept constant at 10 rad(Si)/s. From Figure 2a, one can see that, with the increase in the total dose, the curves of φ_s–V_g show an apparent leftward shift, indicating that the point of voltage amplification ($G = \partial\varphi_s/\partial V_g$) shifts left, which is shown in Figure 2b. This is undesirable in logic devices. In order to understand this phenomenon well, the relationship between ferroelectric capacitance (C_{fe}) and gate voltage is also illustrated in Figure 2c. From Figure 2c, it is found that the ferroelectric capacitance appears to have negative values, resulting in the voltage amplification in Figure 2a. Interestingly, with the total dose increasing from 0 rad to 2 Mrad, the point where the negative capacitance occurs also moves to the left. This is the reason the point of voltage amplification shifts to the left. Additionally, it can be seen from the transfer characteristics that the point for the appearance of the steep subthreshold slope shifts left with the increase in total dose, which is shown in Figure 2d. This is owing to the left shift of the point for the appearance of the negative capacitance on the C_{fe}–V_g curve, which is shown in Figure 2c.

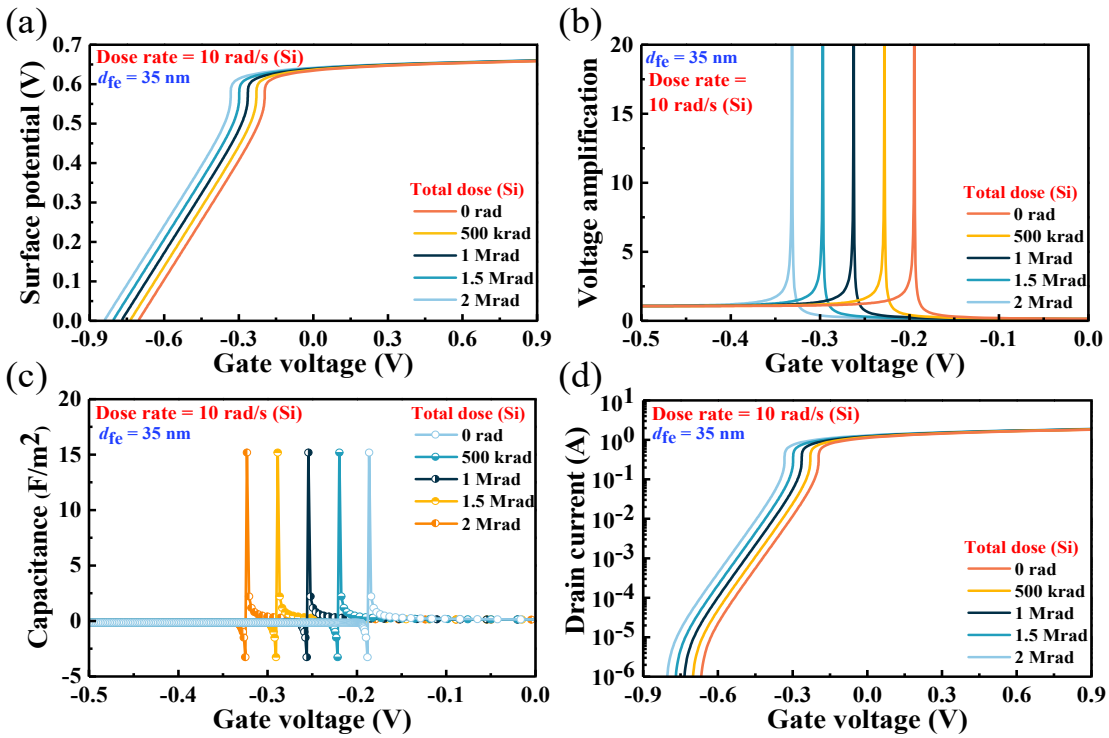

Figure 2. (Color online) (**a**) Silicon surface potential versus gate voltage; (**b**) voltage gain versus gate voltage; (**c**) ferroelectric capacitance versus gate voltage; (**d**) transfer characteristics with different total doses.

In order to understand well the effect of ionizing radiation on the properties of NC-MFIS-FETs, we also investigated the dose rate effect on the electrical characteristics of NC-MFIS-FETs. In the simulating process, the total dose was assumed to be 500 krad. Figure 3a–d present the silicon surface potential (φ_s), voltage gain ($G = \partial\varphi_s/\partial V_g$), ferroelectric capacitance (C_{fe}), and drain current (I_{ds}) as a function of gate voltage (V_g), respectively. As seen in Figure 3a, the φ_s–V_g curve shows a leftward shift with the increasing dose rate, leading to a leftward shift in the boost transition point. The results indicated that there is a decrease in the surface potential when the dose rate increases. It is due to the ionizing particles that create trapped charges in the insulating layer of the device. The trapped charges can be attributed to the presence of acceptor-like traps that possess energy

levels located below the conduction band, thereby facilitating the capture of electrons. The trapped charges in the insulating layer can reduce the effectiveness of the gate voltage in controlling the drain current through the device. However, there is nearly no influence on the capability of step-up conversion, which can be confirmed from Figure 3b. It should be noted that, with the increase in dose rate, the value of negative capacitance shows a slight increase trend, which is shown in Figure 3c. Even so, it has little effect on the steep switching in the transfer characteristic curve, as shown in Figure 3d. It is worthy paying attention to the fact that the driving current decreases with the increasing dose rate; the result can also be understood from the doping effect, just like the result modeled by Liu et al. [32]. They derived that the drain current decreases as the channel doping concentration increases.

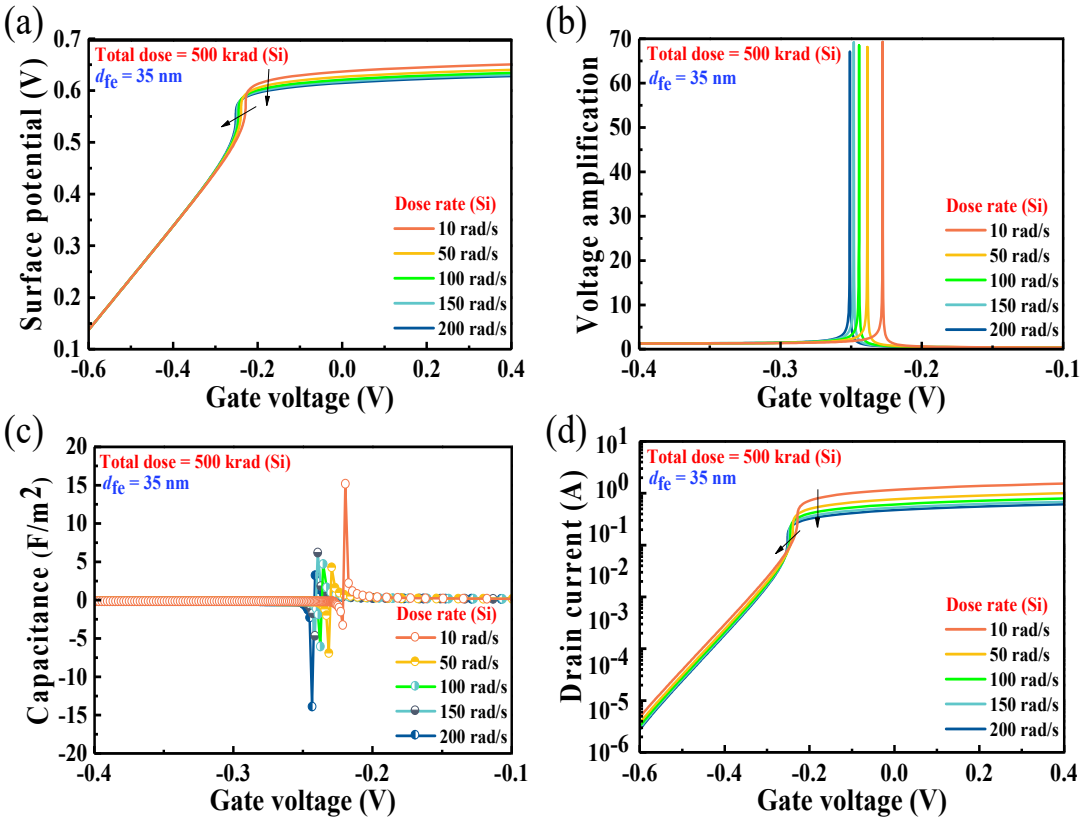

Figure 3. (Color online) (**a**) Silicon surface potential versus gate voltage, (**b**) voltage gain versus gate voltage, (**c**) ferroelectric capacitance versus gate voltage, and (**d**) transfer characteristics with different total dose rates.

For the purpose of further understanding the effect of ionizing radiation on the electrical properties of NC-MFIS-FETs, the C_{fe}–V_g curves for various ferroelectric thicknesses (range from 10 nm to 50 nm) are presented in Figure 4. The total dose and dose rate were assumed to be 500 krad (Si) and 10 rad/s (Si), respectively. For comparison, the results of C_{fe}–V_g before irradiation for different ferroelectric thicknesses were also illustrated. The solid lines stand for the results before irradiation, while the dash lines denote the results after irradiation. It is interesting that, for a fixed d_{fe}, the positive capacitance will increase, while the negative capacitance will decrease after irradiation. Additionally, after irradiation, there is a leftward shift for the curve of C_{fe}–V_g, and the shift becomes more obvious as the thickness of the ferroelectric film increases. This result indicated that the relatively thin ferroelectric thin film is beneficial to reduce the effect of irradiation.

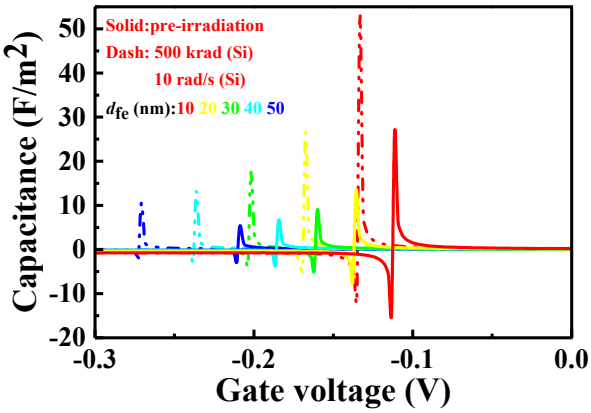

Figure 4. (Color online) Ferroelectric capacitance of MFIS-NCFET with different ferroelectric layers before irradiation and under fixed irradiation.

4. Conclusions

In summary, we developed a total dose as well as a dose rate model for NC-MFIS-FETs. Based on this model, the effects of irradiation on the surface potential, ferroelectric capacitance, voltage gain, and transfer characteristics of NC-MFIS-FET were investigated. The results show that the surface potential, ferroelectric capacitance, voltage gain, and transfer characteristics show a negative drift with the increasing total dose, which is caused by the fixed charge of the ferroelectric layer and the trapped charge of the insulating layer owing to irradiation, while the amplitude of drain current decreases with the increasing dose rate, which is owing to the decrease in the surface potential caused by the accumulation of electrons generated by irradiation on the silicon surface. It is expected that this result may help to elucidate the irradiation mechanism of NC-FETs and provide valuable information for researchers and practitioners for designing and optimizing NCFET devices for use in radiation-prone environments. This proposed model can be integrated into circuit simulators to predict the radiation response of NCFET-based circuits, providing valuable insights for developing radiation-hardened techniques for negative capacitance field-effect transistors.

Author Contributions: Writing—original draft preparation, Y.X. and X.D.; writing—review and editing, H.C., K.X., G.L. and M.T. All authors have read and agreed to the published version of the manuscript.

Funding: The authors would like to thank the financial support from the cultivation projects of the National Major R & D Project (grant no. 92164108), the National Natural Science Foundation of China under Grant Nos. 51872250 and 11835008, the technology innovation leading plan (Science and technology tackling) project of Hu nan Provincial new and high-tech industry under Grant No. 2020GK2052, the State Key Laboratory of Intense Pulsed Radiation Simulation and Effect (North west Institute of Nuclear Technology) under Grant No. SKLIPR1814, the Foundation of Innovation Center of Radiation Application (grant no. KFZC2020020901), and the Key Laboratory of Low Dimensional Materials and Application Technology of Ministry of Education (Xiang tan University) under Grant No. KF20180203.

Institutional Review Board Statement: Not applicable.

Informed Consent Statement: Not applicable.

Data Availability Statement: All data included in this study are available upon request by contact with the corresponding author.

Conflicts of Interest: The authors declare no conflict of interest.

References

1. Salahuddin, S.; Datta, S. Use of negative capacitance to provide voltage amplification for low power nanoscale devices. *Nano Lett.* **2008**, *8*, 405–410. [CrossRef] [PubMed]
2. Khan, A.I.; Chatterjee, K.; Wang, B.; Drapcho, S.; You, L.; Serrao, C.; Bakaul, S.R.; Ramesh, R.; Salahuddin, S. Negative capacitance in a ferroelectric capacitor. *Nat. Mater.* **2015**, *14*, 182–186. [CrossRef] [PubMed]
3. Gao, W.; Khan, A.; Marti, X.; Nelson, C.; Serrao, C.; Ravichandran, J.; Ramesh, R.; Salahuddin, S. Room-temperature negative capacitance in a ferroelectric–dielectric superlattice heterostructure. *Nano Lett.* **2014**, *14*, 5814–5819. [CrossRef]
4. Cheng, P.H.; Yin, Y.T.; Tsai, I.N.; Lu, C.H.; Li, L.J.; Pan, S.C.; Shieh, J.; Shiojiri, M.; Chen, M.J. Negative capacitance from the inductance of ferroelectric switching. *Commun. Phys.* **2019**, *2*, 32. [CrossRef]
5. Hoffmann, M.; Fengler, F.P.G.; Herzig, M.; Mittmann, T.; Max, B.; Schroeder, U.; Negrea, R.; Lucian, P.; Slesazeck, S.; Mikolajick, T. Unveiling the double-well energy landscape in a ferroelectric layer. *Nature* **2019**, *565*, 464–467. [CrossRef] [PubMed]
6. Zubko, P.; Wojdeł, J.C.; Hadjimichael, M.; Fernandez-Pena, S.; Sené, A.; Luk'yanchuk, I.; Triscone, J.-M.; Íñiguez, J.J.N. Negative capacitance in multidomain ferroelectric superlattices. *Nature* **2016**, *534*, 524–528. [CrossRef]
7. Hoffmann, M.; Khan, A.I.; Serrao, C.; Lu, Z.; Salahuddin, S.; Pešić, M.; Slesazeck, S.; Schroeder, U.; Mikolajick, T. Ferroelectric negative capacitance domain dynamics. *J. Appl. Phys.* **2018**, *123*, 184101. [CrossRef]
8. Yadav, A.K.; Nguyen, K.X.; Hong, Z.; García-Fernández, P.; Aguado-Puente, P.; Nelson, C.T.; Das, S.; Prasad, B.; Kwon, D.; Cheema, S.J.N. Spatially resolved steady-state negative capacitance. *Nature* **2019**, *565*, 468–471. [CrossRef]
9. Tsai, M.-J.; Chen, P.-J.; Hsu, C.-C.; Ruan, D.-B.; Hou, F.-J.; Peng, P.-Y.; Wu, Y.-C. Atomic-level analysis of sub-5-nm-thick $Hf_{0.5}Zr_{0.5}O_2$ and characterization of nearly hysteresis-free ferroelectric FinFET. *IEEE Electron Device Lett.* **2019**, *40*, 1233–1236. [CrossRef]
10. Lee, S.Y.; Chen, H.W.; Shen, C.H.; Kuo, P.Y.; Chung, C.C.; Huang, Y.E.; Chen, H.Y.; Chao, T.S. Experimental Demonstration of Stacked Gate- All-Around Poly-Si Nanowires Negative Capacitance FETs With Internal Gate Featuring Seed Layer and Free of Post-Metal Annealing Process. *IEEE Electron Device Lett.* **2019**, *40*, 1708–1711. [CrossRef]
11. Si, M.; Jiang, C.; Su, C.-J.; Tang, Y.-T.; Yang, L.; Chung, W.; Alam, M.; Ye, P. Sub-60 mV/dec ferroelectric HZO MoS_2 negative capacitance field-effect transistor with internal metal gate: The role of parasitic capacitance. In Proceedings of the 2017 IEEE International Electron Devices Meeting (IEDM), San Francisco, CA, USA, 2–6 December 2017; pp. 23.5. 1–23.5. 4.
12. Zhou, J.; Han, G.; Li, Q.; Peng, Y.; Lu, X.; Zhang, C.; Zhang, J.; Sun, Q.-Q.; Zhang, D.W.; Hao, Y. Ferroelectric HfZrO*x* Ge and GeSn PMOSFETs with Sub-60 mV/decade subthreshold swing, negligible hysteresis, and improved I_{ds}. In Proceedings of the 2016 IEEE International Electron Devices Meeting (IEDM), San Francisco, CA, USA, 3–7 December 2016; pp. 12.2.1–12.2.4.
13. Saha, A.K.; Datta, S.; Gupta, S.K. "Negative capacitance" in resistor-ferroelectric and ferroelectric-dielectric networks: Apparent or intrinsic? *J. Appl. Phys.* **2018**, *123*, 105102. [CrossRef]
14. Kwon, D.; Liao, Y.-H.; Lin, Y.-K.; Duarte, J.P.; Chatterjee, K.; Tan, A.J.; Yadav, A.K.; Hu, C.; Krivokapic, Z.; Salahuddin, S. Response speed of negative capacitance FinFETs. In Proceedings of the 2018 IEEE Symposium on VLSI Technology, Honolulu, HI, USA, 18–22 June 2018; pp. 49–50.
15. Krivokapic, Z.; Rana, U.; Galatage, R.; Razavieh, A.; Aziz, A.; Liu, J.; Shi, J.; Kim, H.; Sporer, R.; Serrao, C. 14 nm ferroelectric FinFET technology with steep subthreshold slope for ultra low power applications. In Proceedings of the 2017 IEEE International Electron Devices Meeting (IEDM), San Francisco, CA, USA, 2–6 December 2017; pp. 15.1. 1–15.1. 4.
16. Sun, S.L.; Ma, Y.; Zhou, Y.C.; Wu, C.L.; Li, J.C. A numerical model for the leakage characteristics in ferroelectric thin films under ionizing radiation. *Radiat. Eff. Defects Solids* **2014**, *169*, 538–546. [CrossRef]
17. Chong, C.; Liu, H.; Wang, S.; Wu, X. Research on Total Ionizing Dose Effect and Reinforcement of SOI-TFET. *Micromachines* **2021**, *12*, 1232. [CrossRef] [PubMed]
18. Ray, A.; Naugarhiya, A.; Mishra, G.P. Analysis of total ionizing dose response of optimized fin geometry workfunction modulated SOI-FinFET. *Microelectron. Reliab.* **2022**, *134*, 114549. [CrossRef]
19. Cui, X.; Cui, J.-W.; Zheng, Q.-W.; Wei, Y.; Li, Y.-D.; Guo, Q. Bias dependence of total ionizing dose effects in 22 nm bulk nFinFETs. *Radiat. Eff. Defects Solids* **2022**, *177*, 372–382. [CrossRef]
20. Morozzi, A.; Hoffmann, M.; Slesazeck, S.; Mulargia, R.; Robutti, E. TCAD numerical modeling of negative capacitance ferroelectric devices for radiation detection applications. *Solid-State Electron.* **2022**, *194*, 108341. [CrossRef]
21. Bajpai, G.; Gupta, A.; Prakash, O.; Pahwa, G.; Henkel, J.; Chauhan, Y.S.; Amrouch, H. Impact of radiation on negative capacitance finfet. In Proceedings of the 2020 IEEE International Reliability Physics Symposium (IRPS), Dallas, TX, USA, 28 April–30 May 2020; pp. 1–5.
22. Tyagi, K.; Verma, A.; Dutta, A.K. Modeling of the Gate Tunneling Current in MFIS NCFETs. *IEEE Trans. Electron Devices* **2021**, *68*, 5886–5893. [CrossRef]
23. Khan, A.I.; Radhakrishna, U.; Chatterjee, K.; Salahuddin, S.; Antoniadis, D.A. Negative Capacitance Behavior in a Leaky Ferroelectric. *IEEE Trans. Electron Devices* **2016**, *63*, 4416–4422. [CrossRef]
24. Pahwa, G.; Dutta, T.; Agarwal, A.; Khandelwal, S.; Salahuddin, S.; Hu, C.; Chauhan, Y.S. Analysis and Compact Modeling of Negative Capacitance Transistor with High ON-Current and Negative Output Differential Resistance—Part I: Model Description. *IEEE Trans. Electron Devices* **2016**, *63*, 4981–4985. [CrossRef]
25. Pahariya, A.; Dutta, A.K. A New Surface Potential-Based Analytical Model for MFIS NCFETs. *IEEE Trans. Electron Devices* **2022**, *69*, 870–877. [CrossRef]

26. Yan, S.A.; Li, G.; Zhao, W.; Guo, H.X.; Xiong, Y.; Tang, M.H.; Li, Z.; Xiao, Y.G.; Zhang, W.L.; Lei, Z.F.; et al. Ionizing radiation effect on metal–ferroelectric–insulator–semiconductor memory capacitors. *Semicond. Sci. Technol.* **2015**, *30*, 085020. [CrossRef]
27. Chauhan, R.K.; Dasgupta, S.; Chakrabarti, P. A pseudo-two-dimensional model of ann-channel MOSFET under the influence of ionizing radiation. *Semicond. Sci. Technol.* **2002**, *17*, 961–968. [CrossRef]
28. Yan, S.A.; Li, G.; Guo, H.X.; Zhao, W.; Xiong, Y.; Tang, M.H.; Li, Z.; Xiao, Y.G.; Zhang, W.L.; Lei, Z.F. Modeling and simulation of ionizing radiation effect on ferroelectric field-effect transistor. *Jpn. J. Appl. Phys.* **2016**, *55*, 048001. [CrossRef]
29. Batyrev, I.G.; Hughart, D.; Durand, R.; Bounasser, M.; Tuttle, B.R.; Fleetwood, D.M.; Schrimpf, R.D.; Rashkeev, S.N.; Dunham, G.W.; Law, M.; et al. Effects of Hydrogen on the Radiation Response of Bipolar Transistors: Experiment and Modeling. *IEEE Trans. Nucl. Sci.* **2008**, *55*, 3039–3045. [CrossRef]
30. Xiao, Y.G.; Ma, D.B.; Wang, J.; Li, G.; Yan, S.A.; Zhang, W.L.; Li, Z.; Tang, M.H. An improved model for the surface potential and drain current in negative capacitance field effect transistors. *RSC Adv.* **2016**, *6*, 103210–103214. [CrossRef]
31. Sun, J.; Zheng, X.J. Modeling of MFIS-FETs for the Application of Ferroelectric Random Access Memory. *IEEE Trans. Electron Devices* **2011**, *58*, 3559–3565. [CrossRef]
32. Liu, B.L.; Huang, X.Q.; Jiao, Y.X.; Feng, N.; Chen, X.H.; Rong, Z.; Lin, X.N.; Zhang, L.N.; Cui, X.L. Channel doping effects in negative capacitance field-effect transistors. *Solid-State Electron.* **2021**, *186*, 108181. [CrossRef]